



Cite this: RSC Adv., 2018, 8, 24711

## Oscillating Seebeck coefficients in $\pi$ -stacked molecular junctions<sup>†</sup>

Mohsin K. Al-Khaykanee,<sup>id \*ab</sup> Ali K. Ismael,<sup>id ac</sup> Iain Grace<sup>a</sup> and Colin J. Lambert<sup>id \*a</sup>

When a linear aromatic molecule within a nanogap is bound only to a source electrode, and an adjacent molecule is bound only to a drain electrode, the two molecules can interact *via*  $\pi$ - $\pi$  stacking, which allows electrons to flow from the source to the drain, *via*  $\pi$ - $\pi$  bonds. Here we investigate the thermoelectric properties of such junctions, using mono-thiol oligo-phenylene ethynylene (OPE3)-based molecules as a model system. For molecules which are *para*-connected to the electrodes, we show that the Seebeck coefficient is an oscillatory function of the length  $L$  of the  $\pi$ - $\pi$  overlap region and exhibits large positive and negative values. This bi-thermoelectric behavior is a result of quantum interference within the junction, which behaves like a molecular-scale Mach-Zehnder interferometer. For junctions formed from molecular monolayers sandwiched between planar electrodes, this allows both hole-like and electron-like Seebeck coefficients to be realized, by careful control of electrode separation. On the other hand for *meta*-connected molecules, the Seebeck coefficient is insensitive to  $L$ , which may be helpful in designing resilient junctions with more stable and predictable thermoelectric properties.

Received 1st June 2018  
 Accepted 28th June 2018

DOI: 10.1039/c8ra04698k  
[rsc.li/rsc-advances](http://rsc.li/rsc-advances)

## Introduction

Measurement of the Seebeck coefficient  $S$  in single-molecule junctions<sup>1–9</sup> has opened up the possibility of utilizing molecular-scale thin-film materials in flexible thermoelectric devices. A wide variety of single molecules have been measured with reported values of  $S$  up to 100  $\mu\text{V K}^{-1}$ .<sup>9</sup> A key property determining the sign and magnitude of  $S$  is the position of the Fermi energy of the electrodes relative to the middle of the HOMO–LUMO gap of the molecule; a positive  $S$  implies that the Fermi energy  $E_F$  is closer to the highest occupied molecular orbital (HOMO) and a negative  $S$  means it is closer to the lowest unoccupied molecular orbital (LUMO). Recently it has been demonstrated both experimentally and theoretically that single molecules can display bi-thermoelectric behaviour, in which the sign of  $S$  changes in response to both geometric changes<sup>10–12</sup> and the application of pressure,<sup>11</sup> which shift the positions of the HOMO and LUMO transport resonances relative to  $E_F$ . An alternative approach to the control of quantum transport through single molecules involves utilizing quantum interference (QI) of de Broglie waves associated with electrons passing through the molecule,<sup>13–25</sup> which can increase or decrease the

electrical conductance depending on whether QI is constructive or destructive. One type of molecular junction that has shown QI involves two  $\pi$ -stacked molecules,<sup>26–30</sup> as shown in Fig. 1, where each molecule is attached to only one electrode by a thiol anchor and electrons flow from one electrode to the other *via* the overlap between the  $\pi$ -orbitals of the two molecules.

Measurements of the electrical conductance of monothiol-terminated  $\pi$ -stacked oligo-phenylene ethynylene molecules were first reported in,<sup>26</sup> while in,<sup>27</sup> the  $\pi$ -stacking of these molecules was switched on and off using bulky tertiary butyl groups, which controlled the spacing between the  $\pi$  systems of adjacent molecules groups. In<sup>28</sup> it was shown that for  $\pi$ -stacked junctions formed from two amine-terminated conjugated molecules, the conductance, force and flicker noise differ dramatically when compared with the corresponding monomer junctions, thereby highlighting key differences between intra- and inter-molecular charge transport.

In<sup>29</sup> conductance oscillations of  $\pi$  stacked OPE3 with either one (S-OPE3) or two (S-OPE3-S) thiol anchoring groups as a function of their overlap length were measured.  $\pi$ -stacking has also been used to design molecular junctions<sup>30</sup> that either enhance or suppress a phonon transport, while maintaining electrical conductance. In ref. 31 the symmetry breaking effects involved in chemisorbing  $\pi$ -stacked benzene rings to metallic electrodes was shown to have a significant impact on their transport properties. In<sup>32</sup> five representative  $\pi$ -stacked systems were studied to show how conjugation length and substituent groups influence their electrical conductance and Seebeck coefficient. These studies clearly demonstrate that the length of

<sup>a</sup>Department of Physics, University of Lancaster, Lancaster LA1 4YB, UK. E-mail: c.lambert@lancaster.ac.uk; mohsin.kad@gmail.com

<sup>b</sup>Department of Physics, College of Science, University of Babylon, Babel, Iraq

<sup>c</sup>Department of Physics, College of Education for Pure Science, Tikrit University, Tikrit, Iraq

† Electronic supplementary information (ESI) available. See DOI: 10.1039/c8ra04698k



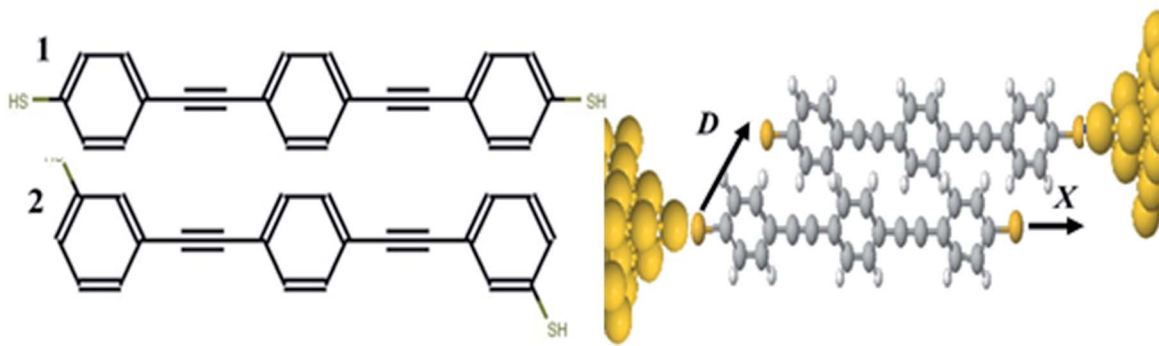


Fig. 1 (Left) Molecular structures for oligophenylene ethynylene (OPE3) molecules with thiol anchor groups connected in the *para* (1) and *meta* (2) position. (Right) An example of a stacking geometry for 1 connected between gold electrodes. The parameters *X* and *D* denote the overlap length and separation respectively.

the overlap region between the two molecules controls the electronic structure of the junction and the nature of the quantum interference.

In this work we investigate whether the ability to tune the transport properties of such pi-stacked junctions can be used to control their Seebeck coefficient. We show that by varying the length of the pi-overlap region, not only can the magnitude of *S* be increased, but also the molecule can display both positive and negative *S*. This bi-thermoelectric behaviour is attractive, because compatible materials with both positive and negative Seebeck coefficients are needed in the construction of useable thermoelectric modules.<sup>33</sup>

## Theoretical methods

To calculate the electronic transport properties of OPE  $\pi$ -conjugated molecules shown in Fig. 1, we use a combination of the density functional code SIESTA<sup>34</sup> and the quantum transport code Gollum.<sup>35</sup> The optimum geometry was calculated for molecules 1 and 2 by relaxing them to a force tolerance of 0.01 eV  $\text{\AA}^{-1}$  using Troullier–Martins pseudopotentials to represent the potentials of the atomic cores,<sup>36</sup> a generalized gradient approximation (GGA–PBE) functional to describe the exchange correlation,<sup>37</sup> double- $\xi$  polarized basis set, and a real-space grid was defined with an energy cutoff 150 Rydberg.

In what follows, we study the effect of varying the pi-overlap length, for molecules with either *para* or *meta* connectivities to the electrodes. The optimal stacking geometry for both molecules was calculated initially without the gold electrodes by altering the displacement *X*, and the inter-molecular spacing *D* of junction containing either *para*-connected molecules 1, or *meta*-connected molecules 2, as shown in Fig. 1 (more details are shown in the ESI†) and then relaxing the dimer to minimize the total energy. We define *X* to be the distance between the sulfur atoms along the axis of the molecule, *i.e.* when *X* = 0 the overlap of the molecule is a maximum. In the case of both OPEs 1 and 2 the optimum values found are *X* = 0.161 nm and *D* = 0.33 nm, and this configuration has a binding energy of –0.77 eV (for binding energies a van der Waals<sup>38</sup> functional was used see Fig. S3 in the ESI†). Within the DFT simulations,

each molecule was then attached to one gold electrode as shown in Fig. 1. The electrodes consist of 6 layers of (111) gold each containing 25 gold atoms, and are terminated by a pyramid of gold atoms. The terminal sulfur atom of the thiol group loses its hydrogen atom when it attaches to a gold electrode, resulting in an optimised gold–sulfur binding distance of 2.4  $\text{\AA}$ . The hydrogen atom of the unattached thiol group remains bound to the sulfur. The zero-bias transmission coefficient *T*(*E*), which is the probability for an electron of energy *E* of electrons to transfer from left-to-right of electrodes<sup>24</sup> was calculated by using the SIESTA code to obtain the DFT mean-field Hamiltonian, and then using Gollum to compute *T*(*E*). The slope of the natural logarithm of the transmission coefficient then yields the Seebeck coefficient *S* via the relation<sup>39</sup>

$$S = \frac{-\pi k_B^2 \tau}{3|e|} \frac{d \ln T(E)}{dE} \Big|_{E=E_F} \quad (1)$$

where  $k_B$  is the Boltzmann constant,  $\tau$  is the temperature of the junction, *e* is the electron charge and  $E_F$  is the Fermi level of the gold electrodes.

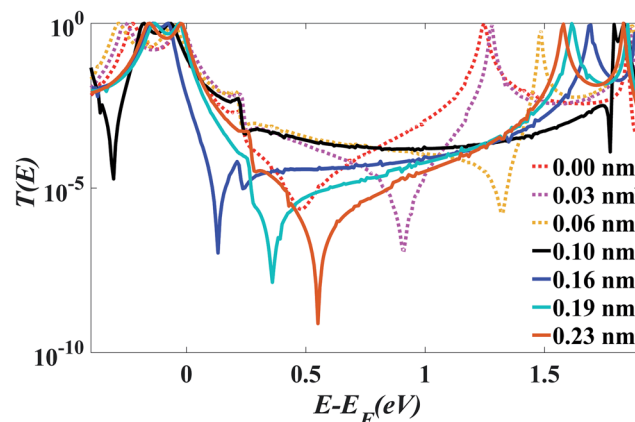


Fig. 2 Zero bias transmission coefficient *T*(*E*) of molecule 1 against electron energy *E* for different displacements *X* and fixed separation *D* = 0.33 nm.

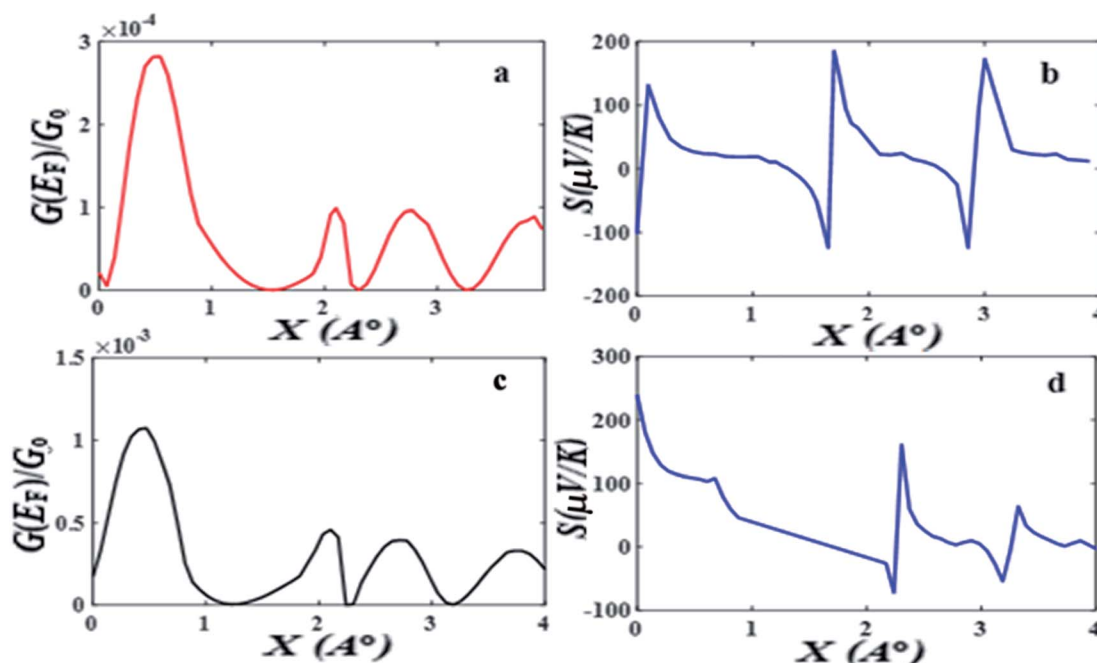


Fig. 3 (a) The electrical conductance and (b) the Seebeck coefficient of pi-stacked OPE3s as a function of displacement when  $E_F = 0.5$  eV relative to the DFT predicted Fermi energy. (c) The electrical conductance and (d) the Seebeck coefficient of pi-stacked OPE3s as a function of displacement when  $E_F = 0.3$  eV relative to the DFT predicted Fermi energy.

## Results and discussions

After choosing the optimum molecule separation of  $D = 0.33$  nm, we varied the displacement  $X$  of the molecule and calculated the transmission coefficient  $T(E)$ . Fig. 2 shows the results for  $X$  varying between 0 and 0.23 nm for the *para* connected molecule **1**, (transmission data for a larger range of  $X$  are presented in the ESI Fig. S6 and S7†). At a value of  $X = 0.161$  nm (which is the optimum stacking geometry) the Fermi energy ( $E - E_F = 0$  eV) lies close to the HOMO resonance, and there is a sharp dip in  $T(E)$  near  $E - E_F = 0.1$  eV in the gap between the HOMO and LUMO transmission resonances. This destructive

interference feature is attributed to the multiple transport paths through the stacked molecule, which cause Mach-Zehnder-type interference effects. Fig. 2 shows that as  $X$  is increased, the anti-resonance moves towards the LUMO resonance and at value of  $X = 0.23$  nm the interference dip sits at  $E - E_F = 0.6$  eV. The transmission curves also show that the HOMO-LUMO gap increases as  $X$  increases, due to the splitting between the two LUMO resonances of the individual molecules, which decreases as the coupling between the two molecules becomes weaker.

Fig. 2 shows when an anti-resonance passes through the Fermi energy, the gradient of  $T(E)$  changes sign, which demonstrates that the Seebeck coefficient  $S$  is sensitive to the

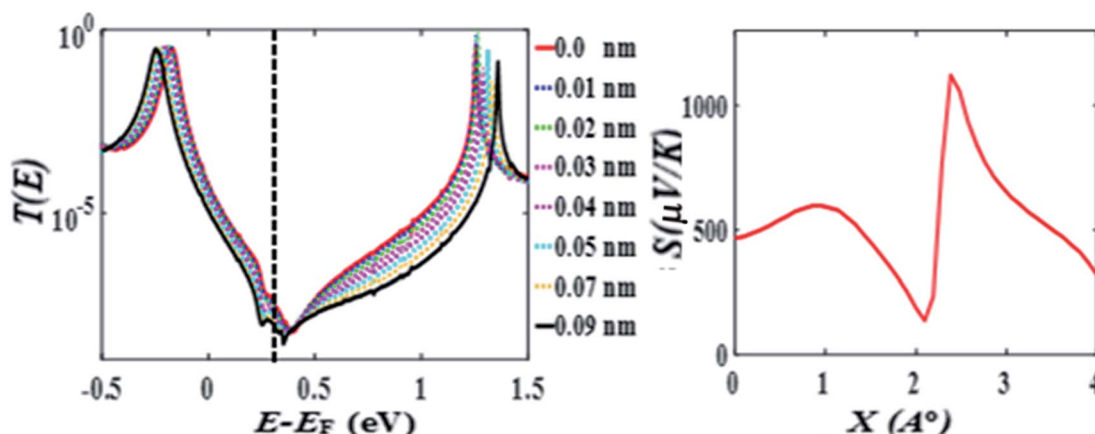


Fig. 4 (Left) Zero bias transmission coefficient  $T(E)$  for molecule **2** for different displacements  $X$  and fixed separation  $D = 0.33$  nm. (Right) Seebeck coefficient  $S$  as a function of overlap length  $X$  ( $D = 0.33$  nm).



stacking geometry. Fig. 3 (right panel) shows the calculated value of  $S$  at room temperature, for a Fermi energy of  $E-E_F = 0.5$  eV (see in Fig. 3(a and b)),  $E-E_F = 0.3$  eV (see in Fig. 3(c and d)), and a separation of  $D = 0.33$  nm for values of  $X$  between 0 and 0.4 nm. At  $X = 0$  the sign of  $S$  is negative and has a magnitude of  $-100 \mu\text{V K}^{-1}$ . As the displacement  $X$  is increased the sign of  $S$  is switched and at a value of  $S$  at  $X = 0.02$  nm is  $100 \mu\text{V K}^{-1}$ . The anti-resonance then moves away from the Fermi energy and  $S$  remains positive with a value of approximately  $25 \mu\text{V K}^{-1}$ . At greater displacements the sign of  $S$  oscillates. Fig. 3 left shows that these oscillations in the sign of  $S$  are accompanied by oscillations in the electrical conductance.

The above calculations were repeated for the *meta*-connected molecule 2 and the results are presented Fig. 4 (the separation is  $D = 0.33$  and the displacement  $X$  is varied between 0 and 0.09 nm). Here the transmission  $T(E)$ , shows an anti-resonance at 0.4 eV, which does not move across the HOMO–LUMO gap as  $X$  is increased. The value of the Seebeck coefficient is therefore positive for all values of  $X$  between 0 and 0.4 nm (see Fig. 4 right panel). This demonstrates that quantum interference effects in the *meta*-connected of molecule 2 are less sensitive to the pi-pi overlap displacement.

## Conclusions

In a previous study of pi-stacked phenyl and anthracene derivatives<sup>32</sup> it was shown that the Seebeck coefficient can change sign by displacing the molecules both parallel and perpendicular to the direction of current flow. Here, we show similar behaviour in linear pi-stacked OPE3 molecules with *para* connectivity to the electrodes, which have been shown to form pi-stacked junctions experimentally,<sup>26</sup> but no such oscillatory behaviour occurs for *meta*-connected OPEs. When molecules are *para*-connected to the electrodes, the location of an anti-resonance due to destructive quantum interference is sensitive to the displacement of the molecules and causes the Seebeck coefficient to alternate in sign. This novel bi-thermoelectric behaviour has the potential to inform the design of thin-film thermoelectric materials and devices based on self-assembled molecular layers, where the spacing between planar electrodes could be controlled by introducing electrically insulating molecules of known length into a film of electrically-active pi-pi stacked molecules, thereby tuning the sign of their Seebeck coefficient. This is important technologically, because junctions with Seebeck coefficients of both signs are needed to boost the thermovoltage. On the other hand when molecules are *meta*-connected to the electrodes, the anti-resonance is less sensitive to the displacement of the molecules and the Seebeck coefficient is consistently positive. This is useful in the design of stable junctions with predictable Seebeck coefficients, since small fluctuations in the electrode separation have little effect.

## Conflicts of interest

There are no conflicts of interest to declare.

## Acknowledgements

This work is supported by the UK EPSRC through grant nos. EP/M014452/1, EP/P027156/1 and EP/N03337X/1. Support from the European Commission is provided by the FET Open project 767187 – QuIET. M. K. A. acknowledges support from the Higher Committee for Education Development, and Babylon University in Iraq. A. K. I. acknowledges financial support from Tikrit University (Iraq).

## References

- 1 L. Rincón-García, C. Evangelí, G. Rubio-Bollinger and N. Agraït, Thermopower measurements in molecular junctions, *Chem. Soc. Rev.*, 2016, **45**(15), 4285–4306.
- 2 L. Cui, R. Miao, C. Jiang, E. Meyhofer and P. Reddy, Perspective: Thermal and thermoelectric transport in molecular junctions, *J. Chem. Phys.*, 2017, **146**(9), 092201.
- 3 P. Reddy, S. Y. Jang, R. A. Segalman and A. Majumdar, Thermoelectricity in molecular junctions, *Science*, 2007, **315**(5818), 1568–1571.
- 4 S. V. Aradhya and L. Venkataraman, Single-molecule junctions beyond electronic transport, *Nat. Nanotechnol.*, 2013, **8**(6), 399.
- 5 A. Tan, J. Balachandran, S. Sadat, V. Gavini, B. D. Dunietz, S. Y. Jang and P. Reddy, Effect of length and contact chemistry on the electronic structure and thermoelectric properties of molecular junctions, *J. Am. Chem. Soc.*, 2011, **133**(23), 8838–8841.
- 6 A. Tan, S. Sadat and P. Reddy, Measurement of thermopower and current–voltage characteristics of molecular junctions to identify orbital alignment, *Appl. Phys. Lett.*, 2010, **96**(1), 013110.
- 7 M. Pfeiffer, A. Beyer, T. Fritz and K. Leo, Controlled doping of phthalocyanine layers by cosublimation with acceptor molecules: A systematic Seebeck and conductivity study, *Appl. Phys. Lett.*, 1998, **73**(22), 3202–3204.
- 8 M. Tsutsui, T. Morikawa, Y. He, A. Arima and M. Taniguchi, High thermopower of mechanically stretched single-molecule junctions, *Sci. Rep.*, 2015, **5**, 11519.
- 9 J. Duan, X. Wang, X. Lai, G. Li, K. Watanabe, T. Taniguchi and E. Y. Andrei, High thermoelectric power factor in graphene/hBN devices, *Proc. Natl. Acad. Sci.*, 2016, **113**(50), 14272–14276.
- 10 J. Vacek, J. V. Chocholoušová, I. G. Stará, I. Starý and Y. Dubí, Mechanical tuning of conductance and thermopower in helicene molecular junctions, *Nanoscale*, 2015, **7**(19), 8793–8802.
- 11 C. M. Finch, V. M. Garcia-Suarez and C. J. Lambert, Giant thermopower and figure of merit in single-molecule devices, *Phys. Rev. B: Condens. Matter Mater. Phys.*, 2009, **79**(3), 033405.
- 12 L. A. Algharagholy, T. Pope and C. J. Lambert, Strain-induced bi-thermoelectricity in tapered carbon nanotubes, *J. Phys.: Condens. Matter*, 2018, **30**(10), 105304.
- 13 L. Rincón-García, A. K. Ismael, C. Evangelí, I. Grace, G. Rubio-Bollinger, K. Porfyrikis and C. J. Lambert,

Molecular design and control of fullerene-based bi-thermoelectric materials, *Nat. Mater.*, 2016, **15**(3), 289.

14 A. K. Ismael, I. Grace and C. J. Lambert, Increasing the thermopower of crown-ether-bridged anthraquinones, *Nanoscale*, 2015, **7**(41), 17338–17342.

15 W. Hong, H. Valkenier, G. Mészáros, D. Z. Manrique, A. Mishchenko, A. Putz and T. Wandlowski, An MCBJ case study: the influence of  $\pi$ -conjugation on the single-molecule conductance at a solid/liquid interface, *Beilstein J. Nanotechnol.*, 2011, **2**, 699.

16 C. M. Guédon, H. Valkenier, T. Markussen, K. S. Thygesen, J. C. Hummelen and S. J. Van Der Molen, Observation of quantum interference in molecular charge transport, *Nat. Nanotechnol.*, 2012, **7**(5), 305.

17 T. Markussen, J. Schiötz and K. S. Thygesen, Electrochemical control of quantum interference in anthraquinone-based molecular switches, *J. Chem. Phys.*, 2010, **132**(22), 224104.

18 Y. Geng, S. Sangtarash, C. Huang, H. Sadeghi, Y. Fu, W. Hong and S. X. Liu, Magic ratios for connectivity-driven electrical conductance of graphene-like molecules, *J. Am. Chem. Soc.*, 2015, **137**(13), 4469–4476.

19 S. Sangtarash, H. Sadeghi and C. J. Lambert, Exploring quantum interference in heteroatom-substituted graphene-like molecules, *Nanoscale*, 2016, **8**(27), 13199–13205.

20 D. Z. Manrique, C. Huang, M. Baghernejad, X. Zhao, O. A. Al-Owaedi, H. Sadeghi and M. R. Bryce, A quantum circuit rule for interference effects in single-molecule electrical junctions, *Nat. Commun.*, 2015, **6**, 6389.

21 G. C. Solomon, C. Herrmann, T. Hansen, V. Mujica and M. A. Ratner, Exploring local currents in molecular junctions, *Nat. Chem.*, 2010, **2**(3), 223.

22 M. Gantenbein, L. Wang, A. A. Al-jobory, A. K. Ismael, C. J. Lambert, W. Hong and M. R. Bryce, Quantum interference and heteroaromaticity of *para*-and *meta*-linked bridged biphenyl units in single molecular conductance measurements, *Sci. Rep.*, 2017, **7**(1), 1794.

23 D. Nozaki and C. Toher, Is the Antiresonance in *Meta*-Contacted Benzene Due to the Destructive Superposition of Waves Traveling Two Different Routes around the Benzene Ring?, *J. Phys. Chem. C*, 2017, **121**(21), 11739–11746.

24 C. J. Lambert, Basic concepts of quantum interference and electron transport in single-molecule electronics, *Chem. Soc. Rev.*, 2015, **44**(4), 875–888.

25 C. J. Lambert and S. X. A. Liu, Magic Ratio Rule for Beginners: A Chemist's Guide to Quantum Interference in Molecules, *Chem.-Eur. J.*, 2018 Mar 20, **24**(17), 4193–4201.

26 S. Wu, M. T. González, R. Huber, S. Grunder, M. Mayor, C. Schönenberger and M. Calame, Molecular junctions based on aromatic coupling, *Nat. Nanotechnol.*, 2008, **3**(9), 569.

27 S. Martín, I. Grace, M. R. Bryce, C. Wang, R. Jitchati, A. S. Batsanov, S. J. Higgins, C. J. Lambert and R. J. Nichols, Identifying diversity in nanoscale electrical break junctions, *J. Am. Chem. Soc.*, 2010, **132**(26), 9157–9164.

28 A. Magyarkuti, O. Adak, A. Halbritter and L. Venkataraman, Electronic and Mechanical Characteristics of Stacked Dimer Molecular Junctions, *Nanoscale*, 2018, **10**(7), 3362–3368.

29 R. Frisenda, V. A. Janssen, F. C. Grozema, H. S. van der Zant and N. Renaud, Mechanically controlled quantum interference in individual  $\pi$ -stacked dimers, *Nat. Chem.*, 2016, **8**(12), 1099.

30 G. Kiršanskas, Q. Li, K. Flensberg, G. C. Solomon and M. Leijnse, Designing  $\pi$ -stacked molecular structures to control heat transport through molecular junctions, *Appl. Phys. Lett.*, 2014, **105**(23), 233102.

31 G. C. Solomon, C. Herrmann, J. Vura-Weis, M. R. Wasielewski and M. A. Ratner, The chameleonic nature of electron transport through  $\pi$ -stacked systems, *J. Am. Chem. Soc.*, 2010 May 20, **132**(23), 7887–7889.

32 Q. Li and G. C. Solomon, Exploring coherent transport through  $\pi$ -stacked systems for molecular electronic devices, *Faraday Discuss.*, 2014, **174**, 21–35.

33 G. S. Nolas, J. Sharp and J. Goldsmid, *Thermoelectrics: basic principles and new materials developments*, Springer Science & Business Media, 2013, p.45.

34 J. M. Soler, E. Artacho, J. D. Gale, A. García, J. Junquera, P. Ordejón and D. Sánchez-Portal, The SIESTA method for *ab initio* order-N materials simulation, *J. Phys.: Condens. Matter*, 2002, **14**(11), 2745.

35 J. Ferrer, C. J. Lambert, V. M. García-Suárez, D. Z. Manrique, D. Visontai, L. Oroszlány and H. Sadeghi, GOLLUM: a next-generation simulation tool for electron, thermal and spin transport, *New J. Phys.*, 2014, **16**(9), 093029.

36 N. Troullier and J. L. Martins, Efficient pseudopotentials for plane-wave calculations, *Phys. Rev. B: Condens. Matter Mater. Phys.*, 1991, **43**(3), 1993.

37 J. P. Perdew, K. Burke and M. Ernzerhof, Generalized gradient approximation made simple, *Phys. Rev. Lett.*, 1996, **77**(18), 3865.

38 L. Dion, H. Rydberg, E. Schröder, D. C. Langreth and B. I. Lundqvist, Van der Waals Density Functional for General Geometries, *Phys. Rev. Lett.*, 2004, **92**(24), 22–25.

39 M. Paulsson and S. Datta, Thermoelectric effect in molecular electronics, *Phys. Rev. B*, 2003, **67**(24), 241403.

